



A Galaxy-targeted Search for the Optical Counterpart of the Candidate NS–BH Merger S190814bv with *Magellan*

S. Gomez¹, G. Hosseinzadeh¹, P. S. Cowperthwaite^{2,10}, V. A. Villar¹, E. Berger¹, T. Gardner³, K. D. Alexander^{4,11}, P. K. Blanchard⁴, R. Chornock⁵, M. R. Drout^{2,6}, T. Eftekhari¹, W. Fong⁴, K. Gill¹, R. Margutti⁴, M. Nicholl^{7,8}, K. Paterson⁴, and P. K. G. Williams^{1,9}

¹ Center for Astrophysics | Harvard & Smithsonian, 60 Garden Street, Cambridge, MA 02138-1516, USA; sgomez@cfa.harvard.edu

² Observatories of the Carnegie Institute for Science, 813 Santa Barbara Street, Pasadena, CA 91101-1232, USA

³ Astronomy Department, University of Michigan, Ann Arbor, MI 48109, USA

⁴ Center for Interdisciplinary Exploration and Research in Astrophysics and Department of Physics and Astronomy, Northwestern University, 2145 Sheridan Road, Evanston, IL 60208-3112, USA

⁵ Astrophysical Institute, Department of Physics and Astronomy, 251B Clippinger Lab, Ohio University, Athens, OH 45701-2942, USA

⁶ Department of Astronomy and Astrophysics, University of Toronto, 50 St. George St., Toronto, Ontario, M5S 3H4, Canada

⁷ Institute for Astronomy, University of Edinburgh, Royal Observatory, Blackford Hill EH9 3HJ, UK

⁸ Birmingham Institute for Gravitational Wave Astronomy and School of Physics and Astronomy, University of Birmingham, Birmingham B15 2TT, UK

⁹ American Astronomical Society, 1667 K Street NW, Suite 800, Washington, DC 20006-1681, USA

Received 2019 August 23; revised 2019 October 3; accepted 2019 October 3; published 2019 October 18

Abstract

On 2019 August 14 the Laser Interferometer Gravitational Wave Observatory (LIGO) and the Virgo gravitational wave interferometer announced the detection of a binary merger, S190814bv, with a low false alarm rate of about 1 in 1.6×10^{25} yr, a distance of 267 ± 52 Mpc, a 90% (50%) localization region of about 23 (5) deg², and a probability of being a neutron star–black hole (NS–BH) merger of >99%. The LIGO/Virgo Collaboration (LVC) defines NS–BH such that the lighter binary member has a mass of $<3 M_{\odot}$ and the more massive one has $>5 M_{\odot}$, and this classification is in principle consistent with a BH–BH merger depending on the actual upper mass cutoff for neutron stars. Additionally, the LVC designated a probability that the merger led to matter outside the final BH remnant of <1%, suggesting that an electromagnetic (EM) counterpart is unlikely. Here we report our optical follow-up observations of S190814bv using the *Magellan* Baade 6.5 m telescope to target all 96 galaxies in the Galaxy List for the Advanced Detector Era catalog within the 50% localization volume (representing about 70% of the integrated luminosity within this region). No counterpart was identified to a median 3σ limiting magnitude of $i = 22.2$ ($M_i \approx -14.9$ mag), comparable to the brightness of the optical counterpart of the binary neutron star merger GW170817 at the distance of S190814bv; similarly, we can rule out an on-axis jet typical of short GRBs. However, we cannot rule out other realistic models, such as a kilonova with only $\sim 0.01 M_{\odot}$ of lanthanide-rich material, or an off-axis jet with a viewing angle of $\theta_{\text{obs}} \gtrsim 15^{\circ}$.

Unified Astronomy Thesaurus concepts: Gravitational waves (678); Neutron stars (1108); Astrophysical black holes (98); Observational astronomy (1145)

1. Introduction

Observing run 3 (O3) of Advanced LIGO and Virgo (ALV) commenced on 2019 April 1, with a 50% increase in sensitivity compared to Observing Runs 1 and 2, corresponding to a binary neutron star merger detection range of about 125 Mpc (Abbott et al. 2016). As of the end of 2019 July the LIGO/Virgo Collaboration (LVC) has issued 22 public alerts (that were not subsequently retracted), of which 18 are high probability binary black hole (BH–BH) mergers, one (S190425z) is a likely binary neutron star (NS–NS) merger, two are ambiguous in terms of their astrophysical nature and overall detection robustness (S190426c and S190510g), and one is likely terrestrial (non-astrophysical) in origin (S190718y). While the candidate event S190426c was initially considered the first possible NS–BH merger, its probability of being such an event is only 13% and its false alarm rate (FAR) is only 1 in 1.6 yr (with a corresponding 14% probability that it is terrestrial in origin).

On 2019 August 14 at 21:10:39 UTC (=58709.88240 MJD), ALV detected a GW candidate event, designated S190814bv, with an incredibly low FAR of 1 in 1.56×10^{25} yr, a luminosity distance of 267 ± 52 Mpc, and a 90% (50%) confidence localization region of 23 (5) deg² (LIGO Scientific Collaboration & Virgo Collaboration 2019a, 2019b); see Figure 1 for the localization map. S190814bv was initially classified with 100% confidence as a “mass-gap” event, namely a merger in which at least one of the binary members is in the mass range 3–5 M_{\odot} . About 13 hr later, initial parameter estimation revised the claimed nature of the event to NS–BH merger (i.e., a merger in which the lightest member has a mass of $<3 M_{\odot}$) with a probability of >99%. We note that this definition allows the event to actually be a BH–BH merger, depending on the actual upper mass cutoff for neutron stars. In addition, the initial parameter estimation indicates that the probability for matter outside of the final merger remnant (the BH) is <1%, suggesting that the merger is unlikely to produce electromagnetic (EM) emission (LIGO Scientific Collaboration & Virgo Collaboration 2019b). We note that this probability encapsulates information from the parameters of the binary (e.g., mass ratio, spin), which are not currently publicly

¹⁰ Hubble Fellow.

¹¹ Einstein Fellow.

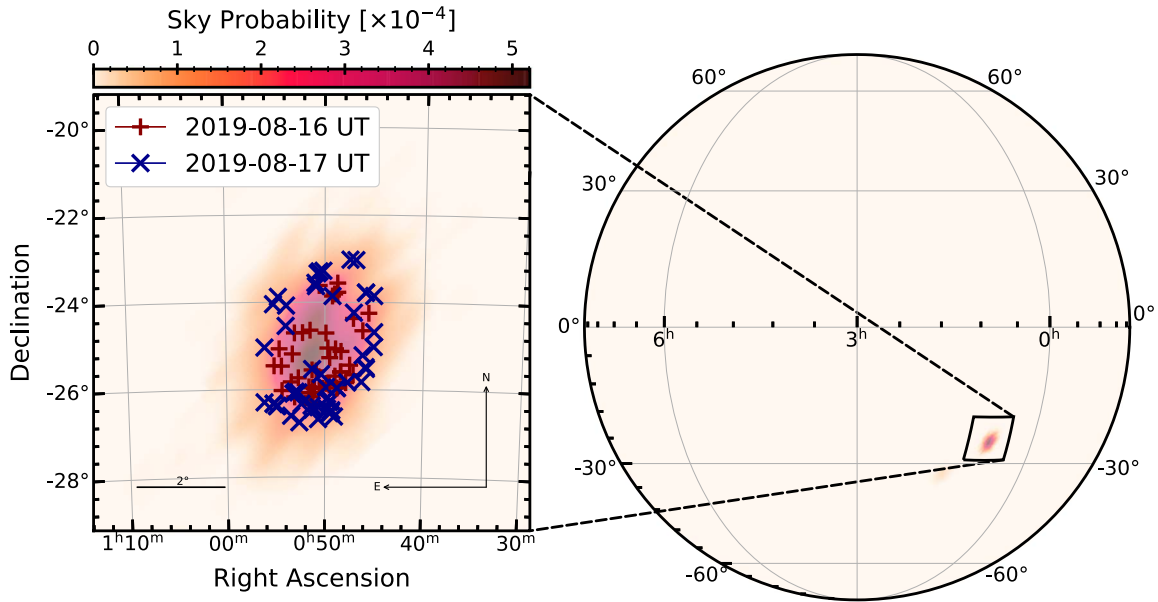


Figure 1. Localization region of S190814bv overlaid with the locations of galaxies observed in our *Magellan* search on 2019 August 16 (red) and 17 (blue). These represent all galaxies present in the GLADE catalog within the 50% localization volume, corresponding to about 50% of all galaxies in this region down to a luminosity of $0.15 L^*$, and about 75% of the integrated galaxy luminosity within the region.

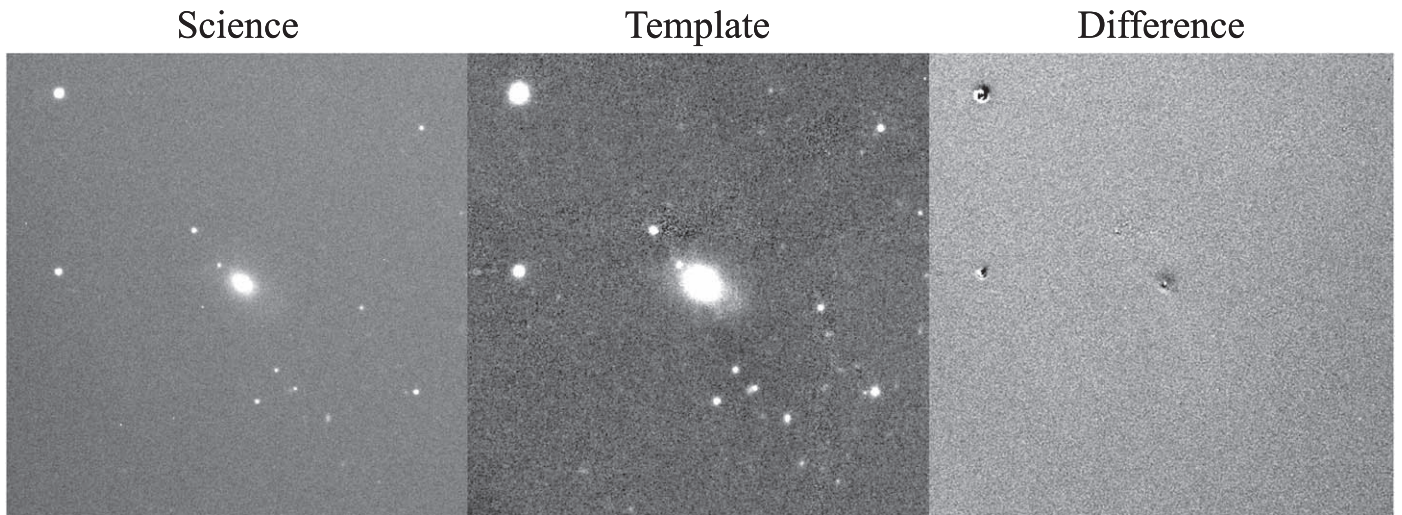


Figure 2. Galaxy imaged with our *Magellan* search in the field of S190814bv (left), along with the corresponding reference image from PS1 3π (middle; Chambers et al. 2016), and the resulting subtraction (right). The images are $2/5$ on a side, oriented with north up and east to the left. The difference image exhibits only astrometric noise and cosmic-ray artifacts; no counterpart is identified in this image to a 3σ limit of $i = 22.2$ mag.

available, and assumptions about the neutron star equation of state.

Here we report our optical follow-up of S190814bv using the *Magellan* Baade 6.5 m telescope to target galaxies within the localization volume. In Section 2 we present our *Magellan* observations. In Section 3 we compare the results of our search to the kilonova emission of GW170817, to theoretical kilonova models, and to on- and off-axis afterglow models. We summarize and draw initial conclusions in Section 4.

2. Galaxy-targeted Follow-up with *Magellan*

Upon receipt of the LVC public alert for S190814bv, our automated software generated a list of galaxies from the Galaxy List for the Advanced Detector Era (GLADE) catalog (Dálya et al. 2018) covering the 90% confidence volume and ranked

by probability within the volume (see Hosseinzadeh et al. 2019 for a detailed discussion).

We commenced follow-up observations with the Inamori-*Magellan* Areal Camera and Spectrograph (IMACS) on the *Magellan* Baade 6.5 m telescope at Las Campanas Observatory in Chile on 2019 August 16 at 08:15:38 UT (35 hr post-merger) and continued until morning twilight, with our last exposure ending at 10:30:02 UT, observing a total of 45 galaxies (Gomez et al. 2019a). On the following night (2019 August 17) we observed from 08:08:39 to 10:27:14 UT (59–61.3 hr post-merger) and imaged 51 additional galaxies (Gomez et al. 2019b); see Figure 1 for the galaxy positions relative to the localization map of S190814bv. We obtained a single 60-s *i*-band image per galaxy to minimize moonlight contamination.

The images were processed in real time following each exposure using a dedicated Python pipeline to perform bias

Table 1
Log of *Magellan* Follow-up Observations

Name	R.A.	Decl.	Date	UT	MJD	Redshift	M_B	Limiting Mag. ^a
2MASX J00494172–2503029	00 ^h 49 ^m 41 ^s .70	–25 ^d 03 ^m 02 ^s .9	2019 Aug 16	08:15:37.9	58711.34418	0.0581	–19.77	22.14
PGC 7877	00 ^h 51 ^m 29 ^s .90	–24 ^d 38 ^m 33 ^s .0	2019 Aug 16	08:21:39.0	58711.34837	0.0612	–20.62	22.15
PGC 777629	00 ^h 51 ^m 17 ^s .80	–25 ^d 33 ^m 13 ^s .6	2019 Aug 16	08:26:24.7	58711.35167	0.0606	–18.59	22.25
PGC 3235511	00 ^h 49 ^m 30 ^s .60	–25 ^d 16 ^m 19 ^s .6	2019 Aug 16	08:29:33.4	58711.35385	0.0585	–18.68	22.42
2MASX J00485495–2504100	00 ^h 48 ^m 55 ^s .00	–25 ^d 04 ^m 10 ^s .1	2019 Aug 16	08:32:12.9	58711.35569	0.0540	–20.04	21.80
PGC 3235463	00 ^h 53 ^m 17 ^s .70	–25 ^d 11 ^m 08 ^s .2	2019 Aug 16	08:35:01.0	58711.35765	0.0577	–18.55	21.78
PGC 786964	00 ^h 49 ^m 53 ^s .50	–24 ^d 42 ^m 25 ^s .9	2019 Aug 16	08:37:56.0	58711.35968	0.0524	–20.06	22.06
ESO 474-035	00 ^h 52 ^m 41 ^s .60	–25 ^d 44 ^m 01 ^s .9	2019 Aug 16	08:40:45.9	58711.36163	0.0605	–20.96	22.23
PGC 786999	00 ^h 53 ^m 04 ^s .60	–24 ^d 42 ^m 15 ^s .8	2019 Aug 16	08:43:55.6	58711.36383	0.0519	–19.80	21.48
PGC 787067	00 ^h 52 ^m 15 ^s .40	–24 ^d 41 ^m 55 ^s .4	2019 Aug 16	08:47:00.8	58711.36597	0.0505	–19.86	22.24
PGC 3235913	00 ^h 51 ^m 36 ^s .60	–25 ^d 56 ^m 31 ^s .9	2019 Aug 16	08:49:49.6	58711.36793	0.0582	–19.38	20.72
PGC 3235862	00 ^h 53 ^m 24 ^s .90	–25 ^d 49 ^m 36 ^s .5	2019 Aug 16	08:52:35.4	58711.36985	0.0579	–19.55	21.77
PGC 777373	00 ^h 50 ^m 52 ^s .40	–25 ^d 34 ^m 37 ^s .4	2019 Aug 16	08:55:27.0	58711.37184	0.0507	–19.49	22.42
PGC 773232	00 ^h 51 ^m 10 ^s .50	–25 ^d 57 ^m 15 ^s .0	2019 Aug 16	08:58:20.0	58711.37384	0.0623	–20.71	21.89
PGC 2864	00 ^h 49 ^m 01 ^s .50	–25 ^d 48 ^m 40 ^s .7	2019 Aug 16	09:01:26.7	58711.37600	0.0525	–21.18	22.16
PGC 3235517	00 ^h 48 ^m 24 ^s .80	–25 ^d 35 ^m 44 ^s .5	2019 Aug 16	09:04:14.4	58711.37794	0.0607	–20.30	22.13
PGC 3235518	00 ^h 48 ^m 22 ^s .50	–25 ^d 36 ^m 05 ^s .0	2019 Aug 16	09:07:01.9	58711.37987	0.0550	–18.97	22.30
PGC 198197	00 ^h 48 ^m 21 ^s .90	–25 ^d 07 ^m 36 ^s .5	2019 Aug 16	09:09:53.7	58711.38186	0.0661	–21.43	22.17
PGC 773004	00 ^h 50 ^m 12 ^s .40	–25 ^d 58 ^m 30 ^s .6	2019 Aug 16	09:12:49.4	58711.38390	0.0608	–19.96	21.39
PGC 198196	00 ^h 47 ^m 28 ^s .90	–25 ^d 26 ^m 26 ^s .4	2019 Aug 16	09:15:42.1	58711.38590	0.0594	–21.36	22.54
PGC 797191	00 ^h 48 ^m 42 ^s .80	–23 ^d 46 ^m 23 ^s .1	2019 Aug 16	09:18:30.3	58711.38785	0.0568	–20.47	21.96
2MASX J00530427–2610148	00 ^h 53 ^m 04 ^s .30	–26 ^d 10 ^m 14 ^s .9	2019 Aug 16	09:21:19.0	58711.38980	0.0545	–20.11	22.20
ESO 474-026	00 ^h 47 ^m 07 ^s .50	–24 ^d 22 ^m 14 ^s .3	2019 Aug 16	09:24:18.2	58711.39188	0.0263	–22.02	21.54
IC 1587	00 ^h 48 ^m 43 ^s .30	–23 ^d 33 ^m 42 ^s .1	2019 Aug 16	09:27:10.7	58711.39387	0.0442	–21.86	22.13
PGC 2998	00 ^h 51 ^m 18 ^s .80	–26 ^d 10 ^m 05 ^s .0	2019 Aug 16	09:30:10.4	58711.39595	0.0635	–20.98	22.44
PGC 773198	00 ^h 50 ^m 32 ^s .90	–25 ^d 57 ^m 25 ^s .9	2019 Aug 16	09:33:01.0	58711.39793	0.0653	–19.69	22.13
PGC 3235917	00 ^h 51 ^m 34 ^s .10	–26 ^d 04 ^m 25 ^s .7	2019 Aug 16	09:35:51.5	58711.39990	0.0653	–18.82	19.98
PGC 3235955	00 ^h 49 ^m 51 ^s .00	–25 ^d 51 ^m 42 ^s .8	2019 Aug 16	09:38:39.9	58711.40184	0.0653	–18.57	19.39
PGC 769203	00 ^h 51 ^m 12 ^s .20	–26 ^d 18 ^m 47 ^s .0	2019 Aug 16	09:41:26.9	58711.40377	0.0587	–20.38	22.19
PGC 133702	00 ^h 48 ^m 58 ^s .30	–25 ^d 41 ^m 36 ^s .4	2019 Aug 16	09:44:16.8	58711.40574	0.0658	–20.67	21.80
2MASX J00511861–2620430	00 ^h 51 ^m 18 ^s .60	–26 ^d 20 ^m 43 ^s .0	2019 Aug 16	09:47:05.2	58711.40770	0.0551	–19.95	22.04
PGC 3235434	00 ^h 53 ^m 09 ^s .20	–25 ^d 27 ^m 20 ^s .5	2019 Aug 16	09:51:01.0	58711.41043	0.0516	–20.63	22.27
PGC 774472	00 ^h 47 ^m 52 ^s .60	–25 ^d 50 ^m 29 ^s .0	2019 Aug 16	09:53:51.3	58711.41240	0.0550	–20.11	22.16
PGC 783013	00 ^h 54 ^m 37 ^s .70	–25 ^d 04 ^m 01 ^s .6	2019 Aug 16	09:56:41.9	58711.41436	0.0499	–20.46	22.26
PGC 798968	00 ^h 50 ^m 34 ^s .50	–23 ^d 37 ^m 06 ^s .8	2019 Aug 16	10:00:06.7	58711.41674	0.0512	–20.51	21.65
PGC 773149	00 ^h 51 ^m 15 ^s .80	–25 ^d 57 ^m 39 ^s .2	2019 Aug 16	10:02:58.3	58711.41873	0.0667	–19.56	21.95
PGC 771842	00 ^h 51 ^m 31 ^s .40	–26 ^d 04 ^m 38 ^s .0	2019 Aug 16	10:05:47.4	58711.42068	0.0656	–20.08	21.53
PGC 3235965	00 ^h 49 ^m 33 ^s .00	–25 ^d 53 ^m 50 ^s .3	2019 Aug 16	10:08:42.4	58711.42271	0.0661	–18.89	20.44
PGC 198252	00 ^h 47 ^m 07 ^s .60	–25 ^d 39 ^m 38 ^s .6	2019 Aug 16	10:11:35.0	58711.42471	0.0598	–20.16	21.61
PGC 2694	00 ^h 46 ^m 10 ^s .40	–24 ^d 39 ^m 00 ^s .7	2019 Aug 16	10:14:28.9	58711.42671	0.0495	–20.91	21.99
PGC 772937	00 ^h 51 ^m 03 ^s .50	–25 ^d 58 ^m 56 ^s .6	2019 Aug 16	10:17:03.2	58711.42851	0.0676	–19.21	22.12
ESO 474-041	00 ^h 54 ^m 24 ^s .30	–25 ^d 27 ^m 50 ^s .6	2019 Aug 16	10:19:37.4	58711.43029	0.0506	–21.42	22.22
PGC 772456	00 ^h 54 ^m 21 ^s .20	–26 ^d 01 ^m 24 ^s .3	2019 Aug 16	10:22:13.5	58711.43209	0.0496	–19.15	22.24
PGC 198243	00 ^h 45 ^m 35 ^s .00	–24 ^d 14 ^m 54 ^s .7	2019 Aug 16	10:24:51.4	58711.43392	0.0516	–19.89	21.75
PGC 2875	00 ^h 49 ^m 14 ^s .70	–23 ^d 51 ^m 30 ^s .8	2019 Aug 16	10:30:01.7	58711.43751	0.0440	–20.68	21.91
PGC 3235867	00 ^h 52 ^m 59 ^s .00	–26 ^d 03 ^m 03 ^s .5	2019 Aug 17	08:08:38.9	58712.33933	0.0670	–19.46	22.08
PGC 2875	00 ^h 49 ^m 14 ^s .70	–23 ^d 51 ^m 30 ^s .8	2019 Aug 17	08:13:23.8	58712.34263	0.0440	–20.68	21.96
IC 1588	00 ^h 50 ^m 57 ^s .70	–23 ^d 33 ^m 28 ^s .8	2019 Aug 17	08:16:19.3	58712.34466	0.0540	–20.67	21.81
PGC 792107	00 ^h 47 ^m 05 ^s .30	–24 ^d 14 ^m 19 ^s .3	2019 Aug 17	08:18:56.4	58712.34648	0.0650	–20.92	22.10
PGC 133715	00 ^h 49 ^m 46 ^s .00	–26 ^d 26 ^m 34 ^s .9	2019 Aug 17	08:21:31.2	58712.34828	0.0543	–21.21	21.81
PGC 3123	00 ^h 53 ^m 11 ^s .80	–26 ^d 05 ^m 38 ^s .3	2019 Aug 17	08:24:10.3	58712.35012	0.0456	–20.58	22.19
PGC 773323	00 ^h 49 ^m 52 ^s .20	–25 ^d 56 ^m 46 ^s .5	2019 Aug 17	08:26:42.2	58712.35188	0.0679	–20.14	21.78
PGC 768565	00 ^h 51 ^m 20 ^s .50	–26 ^d 22 ^m 16 ^s .0	2019 Aug 17	08:29:18.0	58712.35368	0.0501	–19.00	22.42
PGC 771948	00 ^h 52 ^m 41 ^s .90	–26 ^d 04 ^m 04 ^s .3	2019 Aug 17	08:31:50.0	58712.35544	0.0682	–19.40	21.54
PGC 78883	00 ^h 53 ^m 57 ^s .70	–24 ^d 32 ^m 35 ^s .3	2019 Aug 17	08:35:44.3	58712.35815	0.0658	–20.81	21.92
PGC 142558	00 ^h 49 ^m 19 ^s .70	–26 ^d 28 ^m 35 ^s .0	2019 Aug 17	08:38:17.0	58712.35992	0.0567	–20.44	20.08
PGC 3235498	00 ^h 51 ^m 17 ^s .20	–25 ^d 32 ^m 01 ^s .3	2019 Aug 17	08:40:49.6	58712.36168	0.0728	–19.49	21.51
PGC 766121	00 ^h 53 ^m 26 ^s .20	–26 ^d 35 ^m 59 ^s .3	2019 Aug 17	08:43:22.7	58712.36345	0.0624	–20.51	21.80
PGC 769032	00 ^h 52 ^m 22 ^s .30	–26 ^d 19 ^m 44 ^s .9	2019 Aug 17	08:45:57.6	58712.36524	0.0679	–19.26	21.81
PGC 3231	00 ^h 54 ^m 49 ^s .10	–26 ^d 22 ^m 16 ^s .5	2019 Aug 17	08:48:28.4	58712.36699	0.0531	–21.34	22.20
PGC 787272	00 ^h 45 ^m 01 ^s .90	–24 ^d 40 ^m 54 ^s .2	2019 Aug 17	08:51:02.6	58712.36877	0.0514	–19.50	21.94
PGC 765201	00 ^h 50 ^m 40 ^s .80	–26 ^d 40 ^m 36 ^s .8	2019 Aug 17	08:53:41.4	58712.37061	0.0633	–18.75	22.25
PGC 3235993	00 ^h 48 ^m 45 ^s .90	–25 ^d 57 ^m 58 ^s .2	2019 Aug 17	08:56:18.6	58712.37243	0.0700	–19.20	21.47

Table 1
(Continued)

Name	R.A.	Decl.	Date	UT	MJD	Redshift	M_B	Limiting Mag. ^a
PGC 198205	00 ^h 50 ^m 09 ^s .70	−23 ^d 16 ^m 48 ^s .2	2019 Aug 17	08:59:23.5	58712.37457	0.0575	−20.92	22.00
PGC 2798981	00 ^h 55 ^m 12 ^s .90	−26 ^d 19 ^m 51 ^s .5	2019 Aug 17	09:02:22.6	58712.37664	0.0533	−19.99	20.76
PGC 76845	00 ^h 54 ^m 53 ^s .50	−26 ^d 22 ^m 52 ^s .3	2019 Aug 17	09:04:53.2	58712.37839	0.0579	−19.67	22.11
PGC 133703	00 ^h 45 ^m 53 ^s .30	−23 ^d 46 ^m 20 ^s .9	2019 Aug 17	09:07:27.0	58712.38017	0.0526	−21.06	21.77
PGC 133716	00 ^h 49 ^m 27 ^s .60	−26 ^d 32 ^m 17 ^s .9	2019 Aug 17	09:10:05.3	58712.38200	0.0504	−21.39	20.74
PGC 198201	00 ^h 50 ^m 33 ^s .10	−23 ^d 17 ^m 43 ^s .8	2019 Aug 17	09:12:46.7	58712.38387	0.0532	−20.77	22.26
PGC 3235988	00 ^h 49 ^m 03 ^s .00	−26 ^d 37 ^m 07 ^s .1	2019 Aug 17	09:15:44.3	58712.38593	0.0585	−18.81	21.45
2MASX J00455322−2346498	00 ^h 45 ^m 53 ^s .20	−23 ^d 46 ^m 49 ^s .9	2019 Aug 17	09:18:16.2	58712.38769	0.0591	−19.64	22.13
PGC 1337	00 ^h 53 ^m 54 ^s .50	−24 ^d 04 ^m 37 ^s .3	2019 Aug 17	09:20:51.3	58712.38948	0.0471	−20.76	22.22
PGC 801954	00 ^h 50 ^m 44 ^s .70	−23 ^d 40 ^m 19 ^s .8	2019 Aug 17	09:23:21.8	58712.39122	0.0593	−19.81	21.51
PGC 2993	00 ^h 51 ^m 14 ^s .00	−26 ^d 27 ^m 40 ^s .0	2019 Aug 17	09:25:56.0	58712.39301	0.0449	−20.52	22.19
PGC 3236054	00 ^h 46 ^m 17 ^s .20	−25 ^d 49 ^m 26 ^s .4	2019 Aug 17	09:28:35.9	58712.39485	0.0598	−19.98	22.13
PGC 198217	00 ^h 49 ^m 23 ^s .10	−26 ^d 30 ^m 27 ^s .0	2019 Aug 17	09:31:11.0	58712.39666	0.0665	−20.94	21.28
PGC 805757	00 ^h 46 ^m 53 ^s .00	−23 ^d 40 ^m 00 ^s .2	2019 Aug 17	09:33:46.2	58712.39845	0.0559	−20.20	21.65
PGC 198242	00 ^h 45 ^m 03 ^s .60	−25 ^d 01 ^m 11 ^s .2	2019 Aug 17	09:36:32.4	58712.40037	0.0614	−20.62	22.08
2MASX J00502560−2434315 ^b	00 ^h 50 ^m 25 ^s .61	−24 ^d 34 ^m 31 ^s .5	2019 Aug 17	09:38:54.0	58712.40201	0.0392	−21.91	22.06
PGC 3264	00 ^h 55 ^m 13 ^s .50	−26 ^d 19 ^m 16 ^s .5	2019 Aug 17	09:39:06.3	58712.40215	0.0417	−20.54	21.79
PGC 3083	00 ^h 52 ^m 35 ^s .90	−26 ^d 45 ^m 03 ^s .4	2019 Aug 17	09:41:40.8	58712.40394	0.0469	−18.74	21.92
PGC 3235508	00 ^h 50 ^m 23 ^s .70	−25 ^d 38 ^m 58 ^s .9	2019 Aug 17	09:44:24.8	58712.40583	0.0738	−20.14	21.49
PGC 79603	00 ^h 54 ^m 43 ^s .40	−23 ^d 52 ^m 38 ^s .7	2019 Aug 17	09:46:59.3	58712.40763	0.0564	−20.93	21.28
PGC 198221	00 ^h 49 ^m 32 ^s .50	−26 ^d 32 ^m 18 ^s .9	2019 Aug 17	09:49:39.1	58712.40948	0.0670	−19.85	21.89
PGC 774512	00 ^h 47 ^m 42 ^s .60	−25 ^d 50 ^m 15 ^s .3	2019 Aug 17	09:52:11.7	58712.41124	0.0706	−19.30	22.46
PGC 3235964	00 ^h 49 ^m 34 ^s .20	−26 ^d 17 ^m 16 ^s .1	2019 Aug 17	09:55:03.3	58712.41323	0.0709	−19.17	21.27
PGC 783349	00 ^h 56 ^m 06 ^s .70	−25 ^d 02 ^m 08 ^s .2	2019 Aug 17	09:58:20.0	58712.41551	0.0633	−19.75	21.86
PGC 796342	00 ^h 45 ^m 04 ^s .00	−23 ^d 51 ^m 02 ^s .9	2019 Aug 17	10:00:56.4	58712.41731	0.0442	−19.96	21.92
PGC 768185	00 ^h 50 ^m 38 ^s .90	−26 ^d 24 ^m 23 ^s .2	2019 Aug 17	10:03:29.2	58712.41909	0.0707	−21.20	21.85
PGC 798818	00 ^h 50 ^m 54 ^s .40	−23 ^d 37 ^m 54 ^s .8	2019 Aug 17	10:06:19.0	58712.42105	0.0701	−21.25	22.50
PGC 278	00 ^h 47 ^m 28 ^s .20	−23 ^d 01 ^m 22 ^s .8	2019 Aug 17	10:08:54.2	58712.42285	0.0457	−21.20	22.38
PGC 101138	00 ^h 55 ^m 13 ^s .10	−24 ^d 02 ^m 38 ^s .5	2019 Aug 17	10:11:31.6	58712.42466	0.0458	−19.85	22.21
PGC 77801	00 ^h 45 ^m 49 ^s .60	−25 ^d 31 ^m 17 ^s .7	2019 Aug 17	10:14:31.6	58712.42675	0.0650	−18.53	22.13
PGC 3235531	00 ^h 45 ^m 52 ^s .00	−25 ^d 29 ^m 04 ^s .6	2019 Aug 17	10:17:03.6	58712.42851	0.0664	−19.23	22.12
PGC 781464	00 ^h 46 ^m 10 ^s .40	−25 ^d 12 ^m 47 ^s .7	2019 Aug 17	10:19:36.1	58712.43028	0.0703	−19.51	21.55
PGC 769778	00 ^h 49 ^m 22 ^s .50	−26 ^d 15 ^m 32 ^s .9	2019 Aug 17	10:22:07.0	58712.43203	0.0719	−19.08	22.08
PGC 769446	00 ^h 56 ^m 08 ^s .80	−26 ^d 17 ^m 28 ^s .2	2019 Aug 17	10:27:14.3	58712.43558	0.0582	−19.08	22.16

Notes.^a All of the reported magnitudes are corrected for Milky Way extinction.^b GCN circular 25382 accidentally omitted this galaxy.

subtraction and flatfielding. Image subtraction was performed relative to Pan-STARRS1 3π i -band images using the HOTPANTS software (Becker 2015) and we searched for candidate transients through visual inspection. No transient sources were uncovered in these observations to a median 3σ limiting magnitude and 90% percentile range of $i = 22.2_{-0.6}^{+0.3}$. These limits were calculated for each individual image, from a measure of the average sky background and systematic noise sources, calibrated relative to field stars from the PS1 3π catalog. An example of the *Magellan* images and image subtraction results is shown in Figure 2. We provide the information for all of the individual galaxies in Table 1 where the reported magnitudes have been corrected for negligible Galactic extinction with $E(B - V) \approx 0.03$ (Schlafly & Finkbeiner 2011).

The 96 observed galaxies comprise all galaxies from the GLADE catalog in the 50% confidence volume of S190814bv (1.8×10^4 Mpc³) with luminosities of $\gtrsim 0.15 L^*$. To estimate the completeness of this sample we integrate the B -band galaxy luminosity function down to the same limit and estimate an expected 195 galaxies within the 50% localization volume of 1.8×10^4 Mpc³. We adopt values of $M_* = -20.75$,

$\phi_* = 0.0055$, and $\alpha = -1.20$ for the B -band luminosity function $\phi(M) = 0.4 \ln 10 \phi_*^* 10^{L(\alpha+1)} \exp(-10^L)$, where $L = 0.4(M^* - M)$ (Faber et al. 2007). This indicates that in terms of number of galaxies our search was about 50% complete within the 50% confidence region, or equivalently that we covered about 25% of the overall probability of the location of S190814bv. More importantly, in terms of integrated luminosity (and hence roughly stellar mass) the resulting overall fraction is higher, about 35% of the probability (which comprises more than half of the integrated luminosity). We covered every galaxy in the GLADE catalog with $L \geq 0.75 L^*$, a total of 44 galaxies in the 50% localization volume. From integrating the B -band luminosity function down to this luminosity we predict a total of 47 galaxies. Therefore, the GLADE catalog is essentially complete ($\approx 95\%$ coverage) within the 50% volume down to a luminosity of $0.75 L^*$.

3. Comparison to GW170817 and Theoretical Models

At the 90% confidence distance range of S190814bv a kilonova identical to that associated with GW170817 (which peaked at a magnitude of $M_i \approx -15.8$ mag; Villar et al. 2017b) would peak at a magnitude of $i \approx 20.5$ –22 at a timescale of

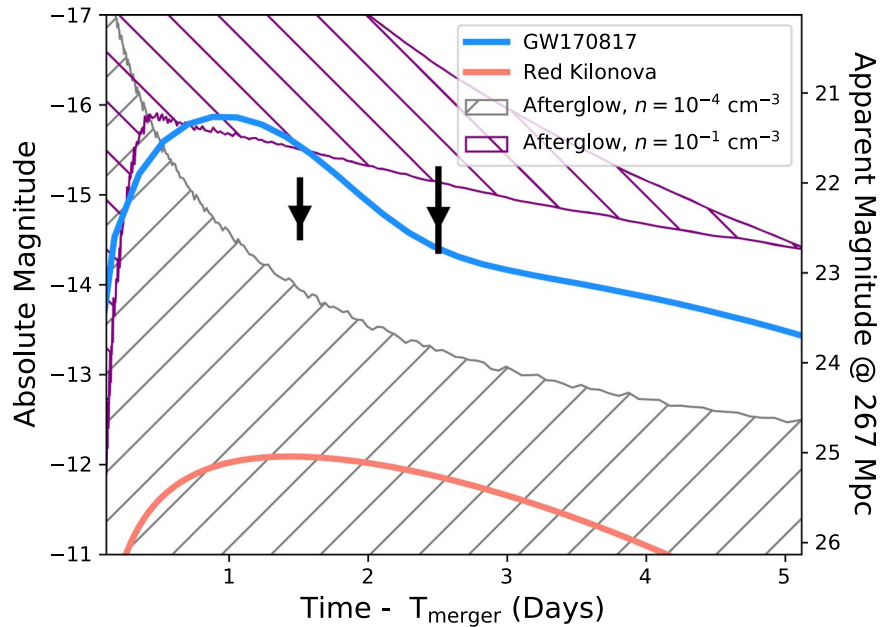


Figure 3. Our *Magellan* search limits compared to several potential optical emission light curve models. The black arrows and lines represent the 90% range for the limiting absolute magnitudes in each night, using the relevant distance of each targeted galaxy. Also shown are the model light curves for the kilonova associated with GW170817 (blue; Villar et al. 2017b), a lanthanide-rich kilonova with an ejecta mass of $0.01 M_{\odot}$ (red), and afterglows based on a range of short GRB properties (Fong et al. 2015) for high density ($n = 10^{-1} \text{ cm}^{-3}$; purple) and low density ($n = 10^{-4} \text{ cm}^{-3}$; gray) environments. The shaded regions represent the span of possible models for different viewing angles, from on-axis jets at the brightest edge of the shaded regions, to an off-axis jet (15° angle) at the bottom edge of the regions. The right-hand-side ordinate shows the relevant apparent magnitudes for the mean distance of S190814bv (267 Mpc) to provide an indication of the rough depth required to detect the various models.

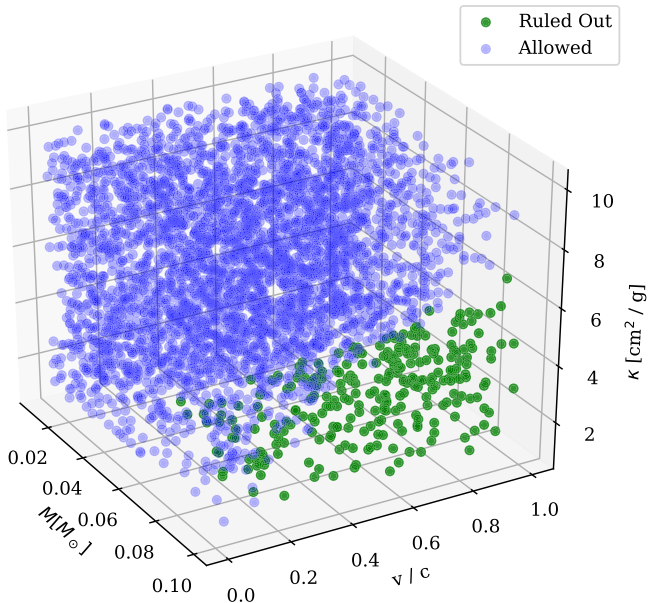


Figure 4. Parameter exploration for variations of the red kilonova model shown in Figure 3. The green points represent the models the satisfy Equation (1), which we can rule out based on our *i*-band upper limits.

about 1 day post-merger; see Figure 3. In said figure we show the best-fit model of GW170817 from Villar et al. (2017b). This is a three component kilonova model, with a “blue” lanthanide-poor component, an intermediate “purple” component, and a “red” lanthanide-rich component; with a respective increasing opacity, spanning $\kappa = 0.5\text{--}10 \text{ cm}^2 \text{ g}^{-1}$, velocities spanning $v_{\text{ej}} = 0.1\text{--}0.26c$, and a total mass of $M_{\text{ej}} \approx 0.078 M_{\odot}$. The limiting magnitudes for our first night of observations span a median and 90% confidence range that can rule out a

GW170817-like kilonova, while the observations obtained on the following night rule out such a kilonova only for the lower half of the distance range.

The kilonova associated with GW170817 was dominated at early time by a bright blue emission component, possibly due to ejecta from the collision interface of the two neutron stars (Metzger & Fernández 2014; Nicholl et al. 2017) or a (short-lived) hypermassive neutron star or magnetar remnant (Fahlman & Fernández 2018; Metzger et al. 2018). In the case of an NS–BH merger such processes are not expected, and the emission will instead be dominated by dynamical ejecta or an accretion disk wind. We therefore compare our limits to a model representative of only the “red” lanthanide-rich component of GW170817 with a nominal ejecta mass of $0.01 M_{\odot}$ and a high opacity of $\kappa = 10 \text{ cm}^2 \text{ g}^{-1}$, which has a peak brightness of $M_i \approx -13 \text{ mag}$ ($i \approx 23.5\text{--}25 \text{ mag}$ at the distance range of S190814bv) on a timescale of about 1–2 days (Figure 3). We find that the resulting models are not significantly affected by the ejecta mass. Such a model cannot be ruled out by our observations for any ejecta mass $< 0.03 M_{\odot}$.

In Figure 3 we show a model with parameters identical to the red component of GW170817 from the model shown in Villar et al. (2017b) ($M_{\text{ej}} = 0.011 M_{\odot}$, $v_{\text{ej}} = 0.137c$, $\kappa = 10 \text{ cm}^2 \text{ g}^{-1}$). We further explore the parameter space of allowed and ruled out models for the red/purple kilonova models, since a blue component would not be expected in a NS–BH merger. We sample 5000 random models in which we allow M_{ej} to vary from 0.01 to $0.1 M_{\odot}$, v_{ej} from 0.0 to $1.0c$, and κ from 1 to $10 \text{ cm}^2 \text{ g}^{-1}$. In Figure 4 we show the set of models that are ruled out by our *i*-band upper limits. We can rule out models that are brighter than either of our 3σ upper limits shown in Figure 3.

The ruled out models satisfy the following equation:

$$-0.124 \frac{\kappa}{cm^2 g^{-1}} + 11.3 \frac{M_{ej}}{M_{\odot}} + 0.886 \frac{v_{ej}}{c} \quad (1)$$

Finally, it is possible that an NS–BH merger can launch a relativistic jet as in short GRBs (Berger 2014; Paschalidis et al. 2015). The currently available GW information does not provide any insight on the inclination angle of the binary, so here we compare to both on- and off-axis models using the median properties of short GRB afterglows (Fong et al. 2015) in the `BOXFIT` software package (van Eerten & MacFadyen 2011). We find that an on-axis afterglow can be ruled out by our observations, while a model with an off-axis viewing angle of $\gtrsim 15^\circ$ will be dimmer than about 24 mag, beyond the limits of our search.

We therefore conclude that for the region covered by our search we can generally rule out an optical counterpart similar to or brighter than GW170817, as well as an on-axis jet typical of cosmological short GRBs. However, we cannot rule out potential scenarios such as low-mass and lanthanide-rich kilonova, or an off-axis jet. We note again that current parameter estimation indicates no matter outside of the remnant’s horizon so it is possible that S190814bv did not produce any EM radiation.

4. Discussion and Conclusions

We presented *Magellan* follow-up observations of the NS–BH merger candidate S190814bv. Our search targeted 96 galaxies in the 50% probability region, and did not yield potential counterparts to a median limiting magnitude of $i \approx 22.2$. We estimate that our search covered about 75% of the integrated galaxy luminosity within the targeted region, leading to about 35% of the effective probability for S190814bv. Within this effective volume we can rule out the presence of an optical counterpart similar to or brighter than GW170817, as well as an on-axis afterglow typical of cosmological short GRBs. We cannot rule out dimmer but relevant models such as a lanthanide-rich kilonova with an ejecta mass of $0.01 M_{\odot}$, or an off-axis jet.

We stress that to robustly rule out the presence of an optical counterpart to S190814bv for this range of models requires coverage of the full localization volume to a limiting magnitude of ≈ 25 mag. This is well beyond the reach of any search reported via the GCN circulars. Thus, the existence of optical emission from S190814bv is likely to remain ambiguous.

From the point of view of GW information for S190814bv, it is unclear whether this is an NS–BH or BH–BH merger since the LVC definition of a neutron star as an object with $< 3 M_{\odot}$ actually allows for both possibilities, depending on the actual mass cutoff for a neutron star. For the purpose of optimizing future EM follow-up of potential NS–BH mergers we urge the LVC to also provide the probability that the lighter binary member has a mass of $< 2 M_{\odot}$, a much better indicator of a true neutron star nature than the current $< 3 M_{\odot}$ definition.

In either case, the LVC has indicated that the probability for matter outside the final BH remnant is negligible ($< 1\%$) suggesting that this is either an NS–BH merger with a high mass ratio and/or negligible black hole spin (in which case the neutron star was not disrupted outside the black hole horizon) or a BH–BH merger. If the latter is the case, then our limit on optical emission (over 35% of the probability volume) is about













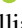

1.8 times deeper than the limit on optical emission from the BH–BH merger GW170814 (at $z \approx 0.12$; Doctor et al. 2017).

The Berger Time-Domain Group is supported in part by NSF grant AST-1714498 and NASA grant NNX15AE50G. P.S.C. is grateful for support provided by NASA through the NASA Hubble Fellowship grant #HST-HF2-51404.001-A awarded by the Space Telescope Science Institute, which is operated by the Association of Universities for Research in Astronomy, Inc., for NASA, under contract NAS 5-26555. V.A.V. acknowledges support from a Ford Foundation Dissertation Fellowship. W.F. and K.P. acknowledge support by the National Science Foundation under grant Nos. AST-1814782 and AST-1909358. This paper includes data gathered with the 6.5 m *Magellan* Telescopes located at Las Campanas Observatory, Chile. `Boxfit` code was supported in part by NASA through grant NNX10AF62G issued through the Astrophysics Theory Program and by the NSF through grant AST-1009863. This research has made use of NASA’s Astrophysics Data System.

Facilities: ADS, *Magellan* (IMACS).

Software: Astropy (Astropy Collaboration 2018), `BOXFIT` (van Eerten & MacFadyen 2011), *healpy* (Zonca et al. 2019), `HOTPANTS` (Becker 2015), `ligo.skymap` (Singer 2019a; Singer et al. 2016), `Matplotlib` (Hunter 2007), *extinction* (Barbary 2016), `NumPy` (van der Walt et al. 2011), `PyGCN` (Singer 2019).

ORCID iDs

S. Gomez  <https://orcid.org/0000-0001-6395-6702>
 G. Hosseinzadeh  <https://orcid.org/0000-0002-0832-2974>
 P. S. Cowperthwaite  <https://orcid.org/0000-0002-2478-6939>
 V. A. Villar  <https://orcid.org/0000-0002-5814-4061>
 E. Berger  <https://orcid.org/0000-0002-9392-9681>
 T. Gardner  <https://orcid.org/0000-0002-3003-3183>
 K. D. Alexander  <https://orcid.org/0000-0002-8297-2473>
 P. K. Blanchard  <https://orcid.org/0000-0003-0526-2248>
 T. Eftekhari  <https://orcid.org/0000-0003-0307-9984>
 W. Fong  <https://orcid.org/0000-0002-7374-935X>
 R. Margutti  <https://orcid.org/0000-0003-4768-7586>
 M. Nicholl  <https://orcid.org/0000-0002-2555-3192>
 K. Paterson  <https://orcid.org/0000-0001-8340-3486>
 P. K. G. Williams  <https://orcid.org/0000-0003-3734-3587>

References

- Abbott, B. P., Abbott, R., Abbott, T. D., et al. 2016, *LRR*, 19, 1
 Astropy Collaboration 2018, *AJ*, 156, 123
 Barbary, K. 2016, *extinction*, v0.3.0, Zenodo, doi:10.5281/zenodo.804967
 Becker, A. 2015, *HOTPANTS*: High Order Transform of PSF And Template Subtraction, Astrophysics Source Code Library, ascl:1504.004
 Berger, E. 2014, *ARA&A*, 52, 43
 Chambers, K. C., Magnier, E. A., Metcalfe, N., et al. 2016, arXiv:1612.05560
 D’Álya, G., Galgóczi, G., Dobos, L., et al. 2018, *MNRAS*, 479, 2374
 Doctor, Z., Kessler, R., Chen, H. Y., et al. 2017, *ApJ*, 837, 57
 Faber, S. M., Willmer, C. N. A., Wolf, C., et al. 2007, *ApJ*, 665, 265
 Fahlman, S., & Fernández, R. 2018, *ApJL*, 869, L3
 Fong, W., Berger, E., Margutti, R., & Zauderer, B. A. 2015, *ApJ*, 815, 102
 Gomez, S., Hosseinzadeh, G., Berger, E., et al. 2019a, GCN, 25366, 1
 Gomez, S., Hosseinzadeh, G., Berger, E., et al. 2019b, GCN, 25382, 1
 Hosseinzadeh, G., Cowperthwaite, P. S., Gomez, S., et al. 2019, *ApJL*, 880, L4
 Hunter, J. D. 2007, *CSE*, 9, 90
 LIGO Scientific Collaboration & Virgo Collaboration 2019a, GCN, 25324, 1
 LIGO Scientific Collaboration & Virgo Collaboration 2019b, GCN, 25333, 1
 Metzger, B. D., & Fernández, R. 2014, *MNRAS*, 441, 3444

- Metzger, B. D., Thompson, T. A., & Quataert, E. 2018, *ApJ*, 856, 101
- Nicholl, M., Berger, E., Kasen, D., et al. 2017, *ApJL*, 848, L18
- Paschalidis, V., Ruiz, M., & Shapiro, S. L. 2015, *ApJL*, 806, L14
- Schlafly, E. F., & Finkbeiner, D. P. 2011, *ApJ*, 737, 103
- Singer, L. 2019b, PyGCN, <https://github.com/lpsinger/pygcn>
- Singer, L. 2019a, ligo.skymap, <https://lscsoft.docs.ligo.org/ligo.skymap/>
- Singer, L. P., Chen, H.-Y., Holz, D. E., et al. 2016, *ApJL*, 829, L15
- van der Walt, S., Colbert, S. C., & Varoquaux, G. 2011, *CSE*, 13, 22
- van Eerten, H. J., & MacFadyen, A. I. 2011, *ApJL*, 733, L37
- Villar, V. A., Guillochon, J., Berger, E., et al. 2017b, *ApJL*, 851, L21
- Zonca, A., Singer, L. P., Lenz, D., et al. 2019, *JOSS*, 4, 1298